



## Sorption and diffusion of organic acids through clayrock: Comparison with inorganic anions



R.V.H. Dagnelie<sup>a,\*</sup>, M. Descostes<sup>a,b,1</sup>, I. Pointeau<sup>a,2</sup>, J. Klein<sup>a</sup>, B. Grenut<sup>a,3</sup>, J. Radwan<sup>a,4</sup>, D. Lebeau<sup>c,5</sup>, D. Georgin<sup>d,6</sup>, E. Giffaut<sup>e,7</sup>

<sup>a</sup>CEA, DEN/DANS/DPC/SECR/Laboratory of Radionuclides Migration Measurements and Modelling, F-91191 Gif-sur-Yvette, France

<sup>b</sup>UMR 8587 CEA, Université d'Evry, CNRS, France

<sup>c</sup>CEA, DEN/DANS/DPC/SECR/Laboratory of Radiolysis and Organic Matter, F-91191 Gif-sur-Yvette, France

<sup>d</sup>CEA, DSV/IBITEC-S/SCBM/Laboratory of 14C Labelling, 91191 Gif-sur-Yvette, France

<sup>e</sup>ANDRA, DRD/TR, Parc de la Croix Blanche, 92298 Châtenay-Malabry Cedex, France

### ARTICLE INFO

#### Article history:

Received 10 January 2013

Received in revised form 13 December 2013

Accepted 1 February 2014

Available online 10 February 2014

This manuscript was handled by Laurent Charlet, Editor-in-Chief, with the assistance of Christophe Tournassat, Associate Editor

#### Keywords:

Organic  
Sorption  
Diffusion  
Clay  
EDTA  
Phthalate

### SUMMARY

Organic complexing species are known to affect radionuclide mobility in the environment. The migration behaviour of several organic ligands was evaluated in the context of a proposed French radioactive waste repository in the Callovo-Oxfordian clayrock formation (COx). This study focuses on four anthropogenic acids (ethylenediaminetetraacetate, isosaccharinate, phthalate, oxalate) that are used in the nuclear fuel cycle or that occur as hydrosoluble degradation products of waste materials. Batch sorption and diffusion experiments were performed with COx clayrock samples using <sup>14</sup>C-labelled radiotracers. The observed effective diffusion coefficients were low ( $D_e \sim 1\text{--}6 \times 10^{-12} \text{ m}^2 \text{ s}^{-1}$ ), an order of magnitude lower than that of tritiated water in the same material, and roughly the same as values for inorganic anions such as  $\text{I}^-$ ,  $\text{Cl}^-$  and  $\text{SO}_4^{2-}$ . The observed correlation of  $D_e$  with molecular mass,  $M^{-1/3}$ , differs significantly from that observed for cations. The organic ligands displayed significant affinity for the COx clayrock, with distribution ratios measured in batch experiments,  $R_d = 1\text{--}30 \text{ L kg}^{-1}$ , which are much higher than usually observed for anionic species. While this result was confirmed by through-diffusion experiments, the  $K_d$  values obtained by fitting diffusion modelling were significantly lower than those measured in the batch experiments.

© 2014 Elsevier B.V. All rights reserved.

### 1. Introduction

Clay-rich sedimentary formations (clayrock) are under consideration as potential host rocks for construction of deep geological repositories for long-lived, high and intermediate level radioactive wastes, an example being the Callovo-Oxfordian formation

(Meuse/Haute-Marne, France). The host formation constitutes the principal barrier for limiting radionuclide (RN) transfer towards the biosphere, mainly due to diffusive properties and the capacity of the clayrock to adsorb most radionuclides (Andra, 2005). Organic matter released from containers and waste packages, and subsequent degradation products, can alter RN uptake and transport in the geological barrier, as well as on cement materials used in vault construction (Hakanen and Ervanne, 2006; Read et al., 1998). Many studies have been carried out focusing on the influence of organic ligands on RN solubility, sorption and mobility in cement environments (Stockdale and Bryan, 2013) and in clayrocks (Maes et al., 2011; Poinssot and Geckeis, 2012). Numerous studies are also dedicated to the sorption of small organics on clayey materials (see for example Drouin et al., 2010), but only few data are available on diffusion-driven migration in clayey materials (Martens et al., 2010) studied the migration of <sup>14</sup>C-labelled natural organic matter (NOM) through boom clayrock). Such investigations are, however, crucial in order to assess the actual organic transport through the geosphere.

\* Corresponding author. Tel.: +33 1 69 08 50 41; fax: +33 1 69 08 32 42.

E-mail addresses: [romain.dagnelie@cea.fr](mailto:romain.dagnelie@cea.fr) (R.V.H. Dagnelie), [michael.descostes@areva.com](mailto:michael.descostes@areva.com) (M. Descostes), [ingmar.pointeau@cea.fr](mailto:ingmar.pointeau@cea.fr) (I. Pointeau), [jonathan.klein@cea.fr](mailto:jonathan.klein@cea.fr) (J. Klein), [bernard.grenut@cea.fr](mailto:bernard.grenut@cea.fr) (B. Grenut), [jean.radwan@cea.fr](mailto:jean.radwan@cea.fr) (J. Radwan), [diane.lebeau@cea.fr](mailto:diane.lebeau@cea.fr) (D. Lebeau), [dominique.georgin@cea.fr](mailto:dominique.georgin@cea.fr) (D. Georgin), [eric.giffaut@andra.fr](mailto:eric.giffaut@andra.fr) (E. Giffaut).

<sup>1</sup> Present address: AREVA Mines, R&D Department, F-92084 Paris la Défense, France. Tel.: +33 (0)1 34 95 91 22.

<sup>2</sup> Present address: CEA, DEN/CAD/DTN/SMTM/LMTE, F-13108 Saint Paul lez Durance, France. Tel.: +33 (0) 4 42 25 61 08.

<sup>3</sup> Tel.: +33 (0)1 69 08 73 75.

<sup>4</sup> Tel.: +33 (0)1 69 08 78 20.

<sup>5</sup> Tel.: +33 (0)1 69 08 80 34.

<sup>6</sup> Tel.: +33 (0)1 69 08 75 96.

<sup>7</sup> Tel.: +33 (0)1 46 11 82 02.



carried out at  $22 \pm 2$  °C with a mean solid/liquid ratio of  $62.5 \text{ g L}^{-1}$  for ISA and EDTA and  $50.0 \text{ g L}^{-1}$  for phthalate and oxalate. The sample was spiked with the  $^{14}\text{C}$ -tracer and then agitated in a Turbula mixer for either 24 h or up to 2 months. At the time of sampling, the tubes were centrifuged at  $50,000g$  for 1 h and a fraction of the supernatant was sampled and the tracer activity determined by liquid scintillation counting (Packard TRICARB 2500 with ultima gold™ cocktail from Perkin Elmer) taking radioactive decay into account. The distribution coefficients  $R_d$  ( $\text{mL g}^{-1}$ ) were calculated using the following equation:

$$R_d = \left( \frac{C_0}{C} - 1 \right) \times \frac{V}{m} = \left( \frac{A_0}{A} - 1 \right) \times \frac{V}{m} \quad (1)$$

with  $C_0/C$  being the initial/residual concentration in solution ( $\text{mol L}^{-1}$ );  $A$  (CPM) the activity;  $V$  (mL) the solution volume; and  $m$  (g) the clayrock dry mass.

#### 2.4. Diffusion experiments

The methodology has been detailed in (Bazer-bachi et al., 2006; Descostes et al., 2008). Preparation and equilibration of the diffusion cells were carried out in an anoxic glove box. The experiments were performed at room temperature ( $22 \pm 2$  °C). The through-diffusion cells consists of two polypropylene reservoirs (up and downstream: 175 and 130 mL, respectively), a polypropylene sample holder, two stainless steel filterplates or two polyether ether ketone grids (PEEK). The clayrock disks in the diffusion cells were equilibrated with the porewater solution by contacting for a period of 48 h to 7 day, then replacing the solution in the chambers. This was carried out three times followed by one last equilibration step lasting two weeks which was sufficient to reach equilibrium. The solution was then replaced by a new solution spiked with the desired tracer (initial concentrations and activities are listed in Table 2). Both compartments were periodically sampled and the solution volume was renewed by addition of synthetic water (downstream) or spiked solution (upstream). Solution samples were counted by liquid scintillation counting (Packard TRICARB 2500, with Ultima Gold™ cocktail).

The analysis of the results was based on Fick's second law for one-dimensional reactive transport (Crank, 1975):

$$\frac{\partial C}{\partial t} = \frac{D_e}{\varepsilon_a + \rho K_d} \frac{\partial^2 C}{\partial x^2} = \frac{D_e}{\alpha} \frac{\partial^2 C}{\partial x^2} \quad (2)$$

where  $C$  is the radioactivity per volume unit ( $\text{Bq m}^{-3}$ );  $t$ , the time (s);  $D_e$ , the effective diffusion coefficient ( $\text{m}^2 \text{ s}^{-1}$ );  $\varepsilon_a$ , the diffusion-accessible porosity;  $\rho$ , the bulk dry density ( $\text{kg m}^{-3}$ );  $K_d$ , the sorption distribution ratio ( $\text{m}^3 \text{ kg}^{-1}$ ); and  $\alpha$ , the rock capacity factor (also called apparent porosity). Boundary and initial conditions are the same as those used by Descostes et al. (2008, 2012), except for the decreasing upstream concentration due to diffusion flux. Full analytical solutions for through-diffusion and reservoir-depletion configurations were obtained in the Laplace space. These were subsequently numerically inverted to provide the time-dependent solution (Moridis, 1998). The analysis of the results was performed

**Table 2**

Total concentration and activity of organics introduced in upstream solutions of through-diffusion experiments. The volume of the upstream compartment is  $175 \pm 2$  mL.

Through-diffusion experiment	ISA	EDTA	Phthalate	Oxalate
$[Orga]_{t=0}$ Upstream compartment				
$C_{\text{TOT}}$ ( $\text{mol L}^{-1}$ )	$1.0 \times 10^{-3}$	$27 \times 10^{-3}$	$1.2 \times 10^{-4}$	$1.7 \times 10^{-5}$
$^{14}\text{C}$ ( $\text{MBq L}^{-1}$ )	2.21	5.05	5.15	2.37
$^{14}\text{C}$ ( $\text{MBq}$ )	0.382	0.873	0.891	0.415

by a least-square fitting of the model to the incoming daily flux in the downstream reservoir, using an analytical solution of Eq. (2). This solution was also compared with a numerical solution using the ALLIANCES platform and the CAST3M code (Montarnal et al., 2007). Results from both methods were found to be consistent.

#### 2.5. Electro spray ionization mass spectrometry

The speciation of the dissolved organic molecules was determined by Electro Spray Ionization Mass Spectrometry (ESI-MS, Nogueira et al., 2009) on a LCT Premier equipped with an Electro-Spray source (Micromass, Manchester, UK) in negative W mode. The capillary voltage was set at 2500 V and the sample cone voltage at 30 V. The desolvation and source temperatures were set at 150 and 100 °C respectively. A syringe injection pump (Harvard Apparatus, Cambridge, MA) delivered the solvent at a constant flow rate of  $10 \mu\text{L min}^{-1}$ . Measurements were performed on 10 mM solutions of ISA, EDTA and phthalate, and a saturated solution of oxalate ( $C_{\text{sat}} \sim 2.4 \times 10^{-5} \text{ mol L}^{-1}$ ) in synthetic porewater (pH adjusted between 7 and 8). A volume of 20  $\mu\text{L}$  of these organic solutions was diluted in 2 mL of methanol before measurement. Samples were then directly introduced into the ion source using a 250  $\mu\text{L}$  glass syringe with a stainless steel needle (Hamilton Co., Reno, NV). Data were acquired by operating the data system in a total ion current (TIC) acquisition mode and several scans were summed to obtain the final spectrum.

### 3. Results

#### 3.1. ESI-MS and speciation in solution

Speciation of organic molecules in the porewater solution was calculated using PhreeqC Chemical Code V2.17 (Parkhurst and Appelo, 1999; Gaucher et al., 2006) using Andra's Thermo\_Chimie\_8 database (Duro et al., 2012), completed with selected data on organics from the Minteq V4 PhreeqC database and reference (Hummel et al., 2005). In this section, the fully protonated ISA molecule which only display two labile protons at pH  $\sim 7$ –8 will be noted  $\text{H}_2\text{ISA}$ . The main aqueous species expected in 10 mM solutions of EDTA,  $\text{H}_2\text{ISA}$ , and phthalate are respectively:  $\text{Mg-EDTA}^{2-}/\text{Ca-EDTA}^{2-}$ : 72/28%,  $\text{HISA}^-/\text{CaHISA}^+$ : 92/8%, and  $\text{Phtal.}^{2-}/\text{Mg-Phthal.}^{2-}/\text{Ca-Phthal.}^{2-}/\text{Na-Phthal.}^{2-}$ : 69/12/12/7%. Solutions saturated with oxalate ( $[\text{Ox}] \sim 2 \times 10^{-5} \text{ mol L}^{-1}$ ) present the following species:  $\text{MgOx}$ ,  $\text{CaOx}$ ,  $\text{Ox}^{2-}$ : 53/24/20%. The ratios between species remain almost unchanged when varying parameters such as pH from 7.0 to 8.5,  $\text{CO}_2$  partial pressure from  $10^{-3.5}$  to  $10^{-1.9}$  atm, or total organic concentration from  $10^{-2}$  to  $10^{-9} \text{ mol L}^{-1}$ .

Calculations were compared to the ESI-MS measurements of 10 mM solutions of EDTA, ISA, phthalate, and a saturated solution of oxalate, in artificial porewater. ESI-MS spectra are presented in Fig. 1. The peaks resulting from synthetic pore water are given in supplementary data. The main peaks observed for the EDTA solution correspond to complexed forms with calcium and magnesium,  $[\text{M-EDTA}]^{2-}$ , and possibly sodium. This result confirms the affinity between EDTA and cations leading to negatively charged species complexes. The major species observed for the ISA solution is also anionic, e.g.  $\text{HISA}^-$ , in good agreement with the previous speciation calculations.  $\text{NaISA}^-$  is also observed in the spectra but no thermodynamic data is available to allow taking this species into account.  $\text{CaHISA}^+$  is not observed as the ionization is performed in negative W mode. A single negative species is observed for phthalate, without cation complexation:  $\text{HPhthal}^-$  ( $m/z = 165.51$  uma).  $\text{Phtal}^{2-}$  was not observed at  $m/z = 82.3$  uma. This may come from formation of a weak ion pair with protons in water, or by phthalate protonation during the dilution in methanol. The measurements on

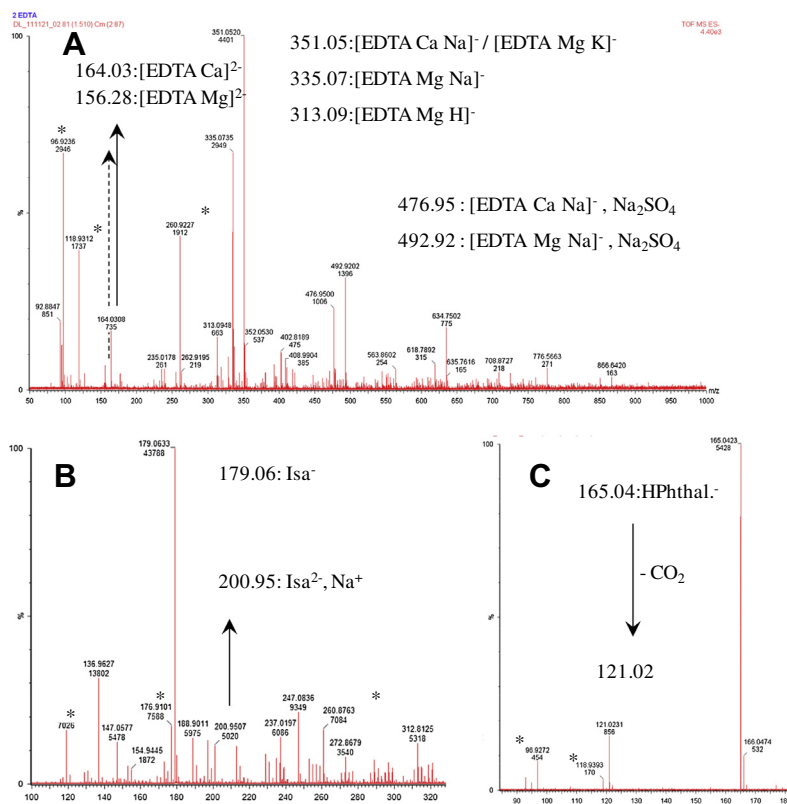


**Fig. 1.** Electro spray ionization mass spectra of organic solutions in porewater solutions. (A) EDTA, 10 mM, (B) ISA, 10 mM, (C) Phthalate, 10 mM. \*Peaks corresponding to ions clusters observed in poral water without organic in negative W mode (anions detection).

oxalate sample gave no signal, even at higher concentration (50  $\mu\text{L}$  in 500  $\mu\text{L}$  of MeOH). This result agrees with the calculation indicating low oxalate solubility and a majority of neutral species (Ca-Ox, Mg-Ox).

Further interpretation is difficult, especially because calculations are limited to complexes with thermodynamic constants available in the literature. Information is particularly rare concerning structures with various cations, e.g.  $[\text{EDTACa/Mg, Na}]^-$  or bigger ion clusters. It is therefore difficult to conclude whether or not such species are representative of the solution or adducts formed during ESI-MS experiment as discussed by Schug and McNair (2003). Still, ESI-MS measurements were performed on samples from the downstream reservoir in diffusion experiments with EDTA and ISA. The results were similar to measurements performed on the upstream compartment indicating that no degradation occurred during the two years experiment. Indeed, it is very unlikely that a degradation of acids occurred by oxidation or bacterial activity leading to  $\text{CO}_2/\text{H}_2\text{O}$  only without molecules displaying an intermediate molecular weight. This also demonstrates that the speciation imposed to acids by the initial porewater was not affected by diffusion through the clayrock.

### 3.2. Sorption experiments

Sorption of organics on COx clayrock was studied as a function of solution concentration. The isotherms,  $R_d(\text{Orga.}) = f[\text{Orga.}]$ , are represented in Fig. 2. The high values observed for  $[\text{Ox.}] > 2.4 \times 10^{-5} \text{ mol L}^{-1}$  correspond to the precipitation of a Ca-Ox solid phase. The results presented are those corresponding to a long period (at least 40 days). This duration ensures that the system reached equilibrium, usually observed within the first 48 h for sorption of organics. Low  $R_d$  values, from 0.1 to 30  $\text{L kg}^{-1}$ , were measured for the range of studied concentrations, but these values

are much higher than sorption usually observed for anions such as  $\text{Cl}^-$ ,  $\text{I}^-$  and  $\text{SO}_4^{2-}$ , on the COx clayrock (Bazer-bachi et al., 2006, 2007; Descostes et al., 2008; Savoye et al., 2012).

The decrease in  $R_d$  values at high concentration is characteristic of the saturation of surface sites. Results over a large concentration range ( $10^{-8}$  to  $10^{-1} \text{ mol L}^{-1}$ ) could be modelled using a one-site Langmuir isotherm. This result is surprising considering the many phases and sorption sites present in the natural material. Such an isotherm is described by Eq. (3)

$$C_{\text{ads}} = S_{\text{max}} \times \frac{K_{\text{ads}} \times C_{\text{eq}}}{1 + K_{\text{ads}} \times C_{\text{eq}}} \quad (3)$$

where  $C_{\text{ads}}$  is the concentration of the adsorbed molecule on the solid phase ( $\text{mol kg}^{-1}$ );  $C_{\text{eq}}$ , the equilibrium concentration in solution ( $\text{mol L}^{-1}$ );  $K_{\text{ads}}$ , the adsorption constant ( $\text{L mol}^{-1}$ ); and  $S_{\text{max}}$  the maximum amount of organic sorbed ( $\text{mol kg}^{-1}$ ) representative of the saturation of surface sites. At low concentrations, i.e. for  $K_{\text{ads}} \times C_{\text{eq}} \ll 1$ , the isotherm becomes linear giving a constant distribution ratio:  $R_d \sim K_{\text{ads}} \times S_{\text{max}}$ . The parameter values obtained by least square fitting of the data are presented in Table 3. Fitting of the oxalate curve gives only one parameter ( $R_d$ ) because CaOx precipitation occurs before saturation of sorption sites. The maximum amount of species sorbed is roughly the same for ISA and phthalate:  $8.8 \times 10^{-4}/9.4 \times 10^{-4} \text{ mol kg}^{-1}$  respectively while a higher value is obtained for EDTA:  $S_{\text{max}} = 2.54 \times 10^{-1} \text{ mol kg}^{-1}$ . Concerning  $R_d$  values, the highest sorption was observed for ISA ( $R_d = 30 \text{ L kg}^{-1}$ ). Phthalate presented the lowest affinity for the clayrock ( $R_d = 1.4 \text{ L kg}^{-1}$ ), which is nevertheless still higher than the usual values for inorganic anions. EDTA and oxalate gave intermediate values, similar to results from other studies, but few data exist for clayey materials (Table 3). Interpretation and physical meaning of the sorption values are discussed in the last section.

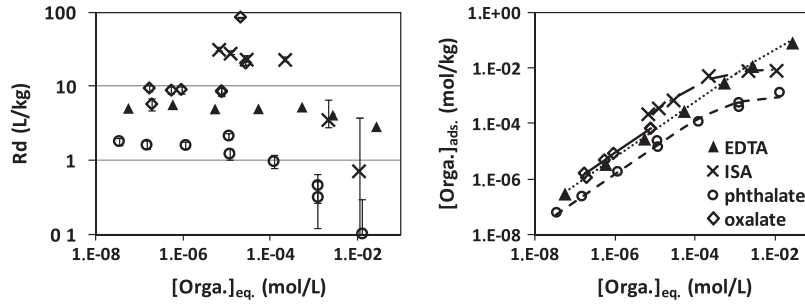


**Fig. 2.** Experimental results for sorption of organic acids, EDTA, ISA, oxalate, phthalate on COx argillite. Sampling time superior to 40 days. (Left) Distribution ratio ( $R_d$ ) as a function of organic concentration at equilibrium. (Right) Experimental concentration of sorbed species ( $\text{mol kg}^{-1}$ ) as a function of concentration in solution ( $\text{mol L}^{-1}$ ) and corresponding results modelled using a Langmuir one-site isotherm.

3.3. Diffusion experiments

Normalised cumulated radioactivities in the downstream compartment ( $Q_{\text{down}}(t)/Q_{\text{up}}(t=0)$ ) and incoming daily fluxes ( $F_{\text{down}}(t) = [Q_{\text{down}}(t+dt) - Q_{\text{down}}(t)]/S \times dt$ ) are given for each ligand in Fig. 3. EDTA was observed in the downstream reservoir after 40 days, much earlier than ISA, which confirms the stronger affinity of ISA for clayrock than EDTA. Results for oxalate and phthalate are very similar indicating little effect of the aromatic ring. Two parameters ( $D_e$  and  $\alpha$ ) can be adjusted by least squares fitting of the flux curves (Fig. 3 and Table 4). Very low effective diffusion coefficients, from 1 to  $5 \times 10^{-12} \text{ m}^2 \text{ s}^{-1}$ , were obtained. These values are at least an order of magnitude lower than that for diffusion of tritiated water. Effective diffusion constants obtained for carboxylic acids in COx clayrock are in the same range as values for inorganic anions like chloride, sulphate or iodide.

The corresponding rock capacity factors range from 0.27 for EDTA to 2.57 for ISA respectively (cf. Table 4). Rock capacity factors previously observed in similar samples for non-sorbing anions were roughly equal to the accessible porosities:  $\varepsilon_a(\text{I}^-, \text{Cl}^-) \sim \alpha(\text{I}^-, \text{Cl}^-) < 0.08$  (Bazer-bachi et al., 2006; Descostes et al., 2008) while the  $\alpha$  values for the carboxylic acids are higher than the total porosity measured with HTO. This result confirms the sorption of organics observed in batch experiments. In the case of sorbing species, the rock capacity factor,  $\alpha$ , obtained by through-diffusion experiment, gives a second estimation of the sorption using Eq. (4):

$$K_d = \frac{(\alpha - \varepsilon_a)}{\rho} \tag{4}$$

where  $K_d$  is the distribution ratio,  $\varepsilon_a$  is the accessible porosity assumed to be the same than that measured for anions  $\varepsilon_a \sim 0.08 \pm 0.02$  and  $\rho \sim 2.4 \text{ kg L}^{-1}$  the clayrock dry density. It was not possible to adjust experimental data with only  $D_e$  as a parameter and ( $K_{\text{ads}}, S_{\text{max}}$ ) taken from batch results. Since a flux curve

allows the adjustment of only two parameters, we then adjusted ( $D_e, \alpha$ ), assuming a linear sorption. In the case of oxalate, ISA and phthalate, upstream concentrations are low ( $< 10^{-3} \text{ mol L}^{-1}$ ), and the use of a constant ( $K_d$ ) instead Eq. (3) gives a reasonable approximation. In the case of EDTA, upstream concentrations are higher and  $K_d$  value obtained by Eq. (4) may slightly underestimate the sorption at trace level. This underestimation does not affect the further discussion.

Values measured by through-diffusion (noted  $K_d$ ) and by batch experiments (noted  $R_d$ ) are compared in Table 4.  $R_d$  and  $K_d$  values follow a similar trend:  $R_d(\text{Cl}^-, \text{I}^-) \ll R_d(\text{EDTA}) < R_d(\text{phthalate}) < R_d(\text{oxalate}) < R_d(\text{ISA})$  for batch experiments and  $K_d(\text{Cl}^-, \text{I}^-) \ll K_d(\text{phthalate}) < K_d(\text{EDTA}) < K_d(\text{oxalate}) < K_d(\text{ISA})$  for diffusion experiments. The only exception is the order of values for EDTA and phthalate which are very close. Unexpectedly high  $R_d/K_d$  ratios, from 6 up to 80, were obtained. These values are much higher than previously observed for anions or cations (Bazer-bachi et al., 2007; Melkior et al., 2005). The origin of such high values is still under investigation and discussed in the next section.

Variations in upstream activity were too small to be exploited. Upstream activities measured during through-diffusion are compared to the model using previous ( $D_e, \alpha$ ) values and presented in Fig. 3. This comparison is used to verify the mass balance during the experiments. A good agreement was observed in the case of phthalate and ISA experiments with less than 1% and 5% differences between experimental data and modelled  $\Delta Q_{\text{up}}$ . The upstream activity for EDTA after 450 days decreased by 14%. This is slightly higher than the 10% expected from modelling and does not affect the determination of diffusive parameters. Only the  $^{14}\text{C}$ -oxalate activity decreased much faster than expected, about 45% in 250 days against the predicted 7%. This decrease affects the measurement by changing the concentration gradient between upstream and downstream compartment. Thus, a second modelling was performed with  $Q_{\text{upstream}} = 0.280 \text{ MBq}$  instead of  $0.406 \text{ MBq}$  in order to prevent an overestimation of transport

**Table 3**

Sorption parameters obtained by modelling the experimental isotherms using a one-site Langmuir model. Results of other studies found in the literature have been included for comparison. Values in bold are solid solution distribution coefficients ( $R_d$ ).

Sorption experiment	ISA	EDTA	Phthalate	Oxalate	Solid phase
Log [ $K_{\text{ads}}$ ( $\text{L} \times \text{mol}^{-1}$ )]	3.54	1.39	3.18	No saturation	COx clayrock
[ $S_{\text{max}}$ ] ( $\text{mol} \times \text{kg}^{-1}$ )	$8.8 \times 10^{-3}$	$2.54 \times 10^{-1}$	$9.4 \times 10^{-4}$		
$R_d = K \times [S_{\text{max}}]$ ( $\text{L} \times \text{kg}^{-1}$ ) (This work)	<b>30</b>	<b>6.2</b>	<b>1.4</b>	<b>8.4</b>	
Pace et al. (2007)		<b>75–100</b> <b>3–5</b> <b>Si<sup>2+</sup> tracer</b>			Clay Sand
Kubicki et al. (1999)			<b>2.5–4.7</b> <b>pH 3/6</b>	<b>Not detailed</b>	Kaolinite, Illite, Montmorillonite
Alliot et al. (2005a,b) Mesuere and Fish (1992)				<b>1–10</b> <b>5–20 × 10<sup>2</sup></b> <b>pH ~ 8</b>	$\alpha$ -alumina Goethite

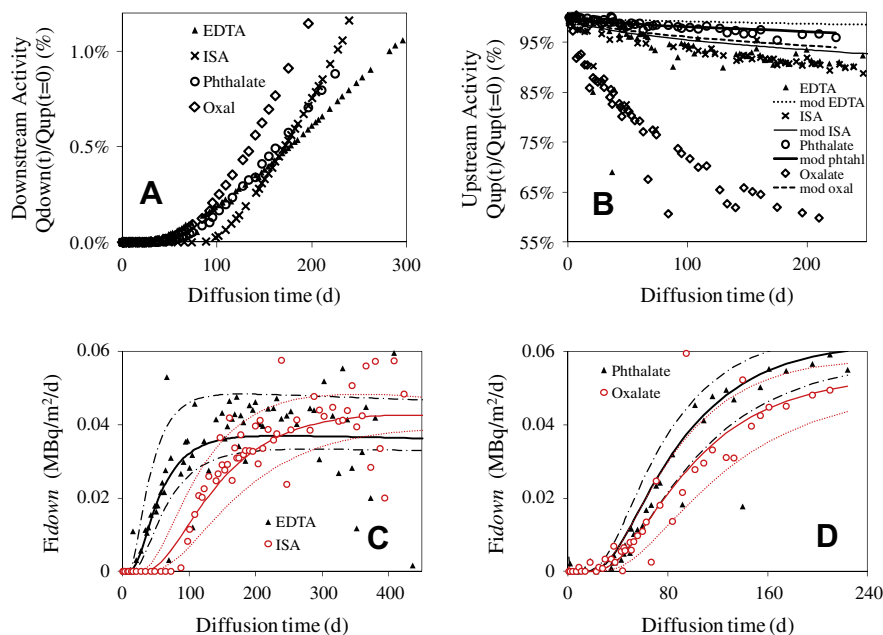


**Fig. 3.** (A and B) Cumulated radioactivities respectively in the downstream ( $Q_{down}$ ) and upstream ( $Q_{up}$ ) compartments of through-diffusion cells. Activities (Bq), were normalised by the initial activity in the upstream compartment  $Q_{up}(t=0)$  in order to compare results from different cells. Curves in (B) represent modelled data, calculated with ( $D_e, \alpha$ ) values taken from downstream flux. (C and D) represent the incoming daily fluxes for  $^{14}\text{C}$ -organics through the clayrock in diffusion cells. Solid curves represent best fit using equation and dotted curves represent adjustment used for the estimation of uncertainties.

**Table 4**  
Diffusive parameters ( $D_e, \alpha$ ) of organic acids, EDTA, ISA, oxalate, phthalate, obtained by through-diffusion experiments. Values in bold refer to the best fit of experimental results. Values between brackets indicate variation in experimental results. The extrapolated  $K_d$  was calculated considering Eq. (4) with  $\varepsilon = 0.08$ ,  $\rho = 2.41 \text{ kg L}^{-1}$ .  $K_d$  values are compared to  $R_d$  values obtained from batch experiments.

	Through-diffusion			Batch
	$D_e$	$\alpha$	$K_d$	$R_d$
Species	$(10^{-12} \text{ m}^2 \text{ s}^{-1})$	(-)	$(\text{L kg}^{-1})$	$(\text{L kg}^{-1})$
EDTA	<b>0.94</b> (0.85–1.23)	<b>0.27</b> (0.27–0.30)	<b>0.08</b>	<b>6.2</b> (5.1–7.0)
ISA	<b>2.8</b> (2.65–3.1)	<b>2.57</b> (2.25–3.10)	<b>1.03</b>	<b>30</b> (14–32)
Phthalate	<b>2.1</b> (1.7–2.3)	<b>0.63</b> (0.60–1.20)	<b>0.23</b>	<b>1.4</b> (1.2–2.0)
Oxalate	<b>3.37</b> (3.2–3.65)	<b>1.76</b> (1.50–2.10)	<b>0.61</b>	<b>8.4</b> (8.2–9.0)
(max.) <sup>b</sup>	(<5.24)	(<2.8)	(<1.11)	
Cl <sup>-a</sup>	<b>4–9</b>	$0.05 < \alpha < 0.09$	$\ll 0.1$	
I <sup>-a</sup>	<b>3–7</b>	$0.07 < \alpha < 0.18$	$< 0.06$	$\ll 0.1$
SO <sub>4</sub> <sup>2-a</sup>	<b>1.9</b>	<b>0.307</b>	<b>0.15 &lt; K<sub>d</sub> &lt; 0.37</b>	<b>0 &lt; R<sub>d</sub> &lt; 0.57 ± 0.16</b>
HTO <sup>a</sup>	24–50	0.16–0.25	$\ll 0.1$	

<sup>a</sup> Taken from (Bazerbachi et al., 2006, 2007; Descostes et al., 2008; Savoye et al., 2012).

<sup>b</sup> Overestimation of oxalate parameters using modified upstream activity.  $Q_{up} = 0.28 \text{ MBq}$  instead of 0.4.

parameters (Table 4). This higher uncertainty in the case of oxalate does not affect the discussion in the last section.

## 4. Discussion

### 4.1. Interpretation of sorption data

A significant sorption of ligands was evidenced by both sorption ( $R_d$ ) and diffusion ( $K_d$ ) experiments. These values confirm the affinity of carboxylic acids for COx clayrock despite the electrostatic repulsion by the negative permanent charge of clayey minerals. The differences between  $R_d$  and  $K_d$  values are still unexplained and several hypotheses may be considered. Among them, the effect of compaction and the enhancement of sorption by creation of new surfaces in crushed rock were discussed by Miller and Wang (2012). The authors suggested that in the case of weak electrostatic interactions, the effective specific surface area is almost identical for crushed and intact rocks. However, this similarity remains un-

clear for species sorbed with stronger interactions. These interactions may alter the chemistry of clay particles and thus the structure and sorption sites available in compacted systems. Other mechanisms to mention are the incorporation of organics in the solid by dissolution/precipitation, the chemical reactivity with NOM, or the slow oxidation of the solid by air ingress during the long-term diffusion experiments.

Another important phenomenon that may partially explain such result is the sorption irreversibility or slow desorption of organics. Adsorption/desorption hysteresis were quantified for numerous organics on soil/sediment systems (Pignatello, 1999). For example sorption of aromatic compounds on sand rich sediment was studied by Kan et al. (1994) indicating that a substantial fraction of the pollutants is bound by strong chemical interactions and resists desorption. Nowara et al. (1997) discussed similar results on carboxylic acids sorbed on soils with various clay contents. They attributed this behaviour to the adsorption between the mineral layers by ionic interactions, especially with montmorillonite. A

mathematical resolution is discussed in (Crank, 1975) in the case of diffusion with various rates,  $\lambda$  and  $\mu$ , for sorption and desorption respectively. If  $\mu = 0$ , the sorption, or chemical reaction, is irreversible and the solid acts as a sink for the solute. If  $\mu \neq 0$ , the flux of solute depends on the ratio  $\mu a^2/D$  (where  $a$  is the diffusion length). The transport is then controlled either by the reversible reaction if  $\mu a^2 \ll D$  or by the diffusion process if  $D \ll \mu a^2$ . In our case, at least two sorption/desorption mechanisms could occur simultaneously, with different rates  $\mu_{\text{irr}}$  (slow or irreversible process)  $\ll \mu_{\text{rev}}$  (fast and reversible process). The observed flux would then correspond to the fraction of solute that diffuses with a fast desorption compared to the time scale of the experiment ( $t = 1 \text{ year}/a = 1 \text{ cm}$ ). Then,  $K_d$  measured by through-diffusion would be representative of the fast and reversible processes, and  $R_d$  measured by batch would represent all sorption processes ( $R_d \gg K_d$ ), including fast, slow and non-reversible mechanisms. This assumption remains to demonstrate and experiments are currently being carried out to quantify the sorption kinetics and hysteresis. It is also crucial to determine if the sorption hysteresis corresponds to a slow desorption or an irreversible incorporation. Smith and Comans (1996) discussed similar issues in the case of  $^{137}\text{Cs}$  remobilisation in sediments. They indeed observed an irreversible sorption of radiocaesium on short-time scale (several months) after a fallout event. However, this “fixed” caesium actually displayed a slow desorption rate and had to be considered explaining long-term environmental mobility of radiocaesium (years).

The macroscopic values obtained in this work may be used for assessing the environmental risk associated with the mobility of organics. Still, these results give no evidences at a microscopic scale. Several mechanisms may be mentioned to describe sorption of organics on mineral surfaces: ion exchange, cation bridging, ligand exchange, van der Waals bonding and hydrophobic effects. Ligand exchange involves the interaction between the carboxylic group and the hydroxyl groups of minerals. It is described as the dominant mechanism for the sorption of NOM on iron oxide (Gu et al., 1994) and for the sorption of carbonic, acetic and oxalic acid on  $\alpha$ -alumina (Alliot et al., 2005b). Van der Waals interactions and ligand exchange were estimated to be responsible for 60% and 35% respectively of the adsorption of organic matter on montmorillonite by Arnarson and Keil (2000). Microscopic-scale characterisation of phthalate sorbed on hematite is given by Hwang et al. (2007), and of oxalate on goethite by Mesuere and Fish (1992). Mono and dicarboxylic acids were also studied on clayey minerals in (Kang and Xing, 2007; Kubicki et al., 1999) and evidences were obtained for both outer-sphere complexes (with weak electrostatic or van der Waals interactions) and inner-sphere complexes (with strong electrostatic or covalent bonds). The possibility of several mechanisms, leading to both strong and weak chemical bounds, would be consistent with the assumption of various rates of desorption. However, given the heterogeneity of clayrocks, further investigations are necessary to evaluate in the first place which phases are driving the sorption of organics on clay.

#### 4.2. Diffusion in clay: anionic exclusion and size dependency

Effective diffusion coefficients for the organics are lower than that for HTO and close to values for anionic tracers such as halides (Table 4). No correlation was observed between the  $D_e$  for carboxylic acids and molecule charge or speciation. The lowest  $D_e$  value was measured for the highest molecular weight ( $M_{\text{Ca-EDTA}} \sim 328 \text{ g mol}^{-1}$ ) and the highest  $D_e$  value for the smallest molecule ( $M_{\text{Ca-Ox}} \sim 112 \text{ g mol}^{-1}$ ). This result leads us to consider the correlation between the size of the species and the diffusion parameters. Size effects in water can be described by a simplified interpretation of Stokes–Einstein law with spherical molecules, leading to Eq. (5)

$$D_0 = r^{-1} \frac{R \times T}{6\pi\eta \times N_a} = M^{-1/3} \frac{R \times T}{6\pi\eta \times N_a \times \left(\frac{3}{4\pi \times N_a \times \rho}\right)^{1/3}} \quad (5)$$

where  $D_0$  is the diffusion coefficient in water ( $\text{m}^2 \text{ s}^{-1}$ ),  $R$  is the universal gas constant,  $T$  the temperature (K),  $\eta$  the viscosity of the medium,  $\rho$  ( $\text{kg m}^{-3}$ ) the density of the molecule,  $N_a$  the Avogadro constant ( $\text{mol}^{-1}$ ),  $r$  (m) and  $M$  ( $\text{kg mol}^{-1}$ ) the hydrated radius and molecular mass of the molecule. One can easily estimate the correlations between size and diffusion using equation  $D_0 = f(r^{-1})$ , or  $D_0 = f(M^{-1/3})$  when the radii of hydrated species are not available.

The ratio:  $D_0(A)/D_0(\text{HTO})$  is useful to discuss the diffusion of solutes in water. The ratio:  $\Pi = [D_e(A)/D_e(\text{HTO})]/[D_0(A)/D_0(\text{HTO})]$  isolates the effect of clay on the diffusion pathway (i.e. tortuosity and constrictivity as discussed by Van Brakel and Heertjes, 1974). Both ratios are represented in Fig. 4 as a function of  $r^{-1}$  or  $M^{-1/3}$  and show two major trends.

Firstly a correlation appears between  $D_0(A^-)/D_0(\text{HTO})$  and  $M^{-1/3}$  for anions. Additional data were added for organics and detailed in supplementary data. Larger/heavy anions display lower diffusion coefficients and small anions diffuse faster. This assumption is verified for many organic species in various solvents (Valencia and González, 2012). For large molecules such as organics, the total charge and the solvation will have less of an effect than the size of the diffusing species. This may explain why the number of negative charges per organic molecule appears to play a rather subordinate role on diffusivity. An exception to this size dependency is observed for halides, for which the strength of the hydration shell strongly affects the motion in water as discussed by (Zhou et al., 2002).

Secondly, the ratio  $\Pi$  is lower than 1, in the range [0.1–0.25] for both organic and inorganic anions. This result is indicative of the anionic exclusion discussed by (Descostes et al., 2008). No clear correlation between  $\Pi$  and  $M^{-1/3}$  is evidenced given the uncertainties and the size effects do not appear to be linked to the clay structure. Results obtained by Melkior et al. (2007) for alkaline cations are given for comparison in (Fig. 4). Diffusion of cations in water is also correlated with hydrated radii. The high values of the ratio  $\Pi$  indicate an enhancement of the macroscopic flux of cations in COx clayrock due to surface mobility of the sorbed cation (Gimmi

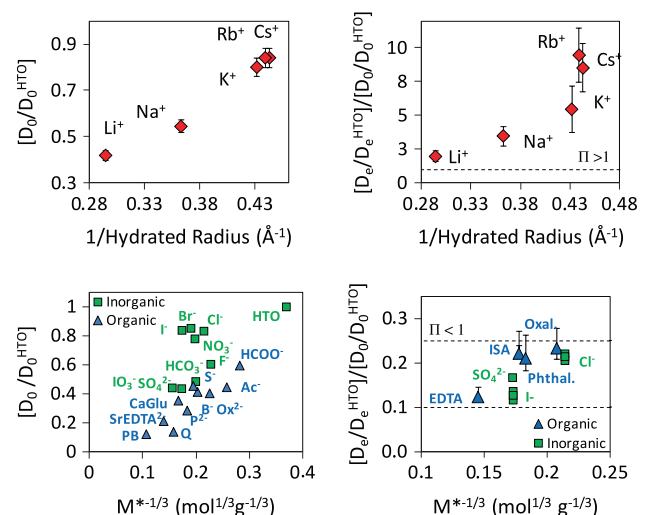


**Fig. 4.** Effect of molecular size and clayrock on ions diffusion. (Left) Diffusion of ions in water ( $D_0/D_0^{\text{HTO}}$ ). (Right) Contribution of COx clayrock to the effective diffusion:  $\Pi = [D_e/D_e^{\text{HTO}}]/[D_0/D_0^{\text{HTO}}]$ . Results are taken from (Bazer-bachi et al., 2006, 2007; Descostes et al., 2008; Savoye et al., 2012) for inorganic anions and from (Melkior et al., 2007; Zheng and Zaoui, 2011) for alkaline cations. The hydration number of inorganic anions was taken into account to calculate molecular mass ( $M'$ ). Additional data added for organics are detailed in supplementary data.

and Kosakowski, 2011). Small cations display more interactions with clay minerals (higher  $K_d$  values) and are more sensitive to the cationic “acceleration”, inducing a correlation between  $\Pi$  and  $r^{-1}$ . Since small values of  $\Pi$  are observed for organics and without correlation, it is likely that almost no surface diffusion occurs despite the significant macroscopic sorption.

## 5. Conclusion

The macroscopic transport parameters of four organics ligands, namely EDTA, ISA, phthalate and oxalate, were measured on COx clayrock. Distribution ratio between solid and liquid was estimated by both sorption in batch and through-diffusion experiments. The organic ligands displayed significant affinity for the COx clayrock. The values measured in batch experiments,  $R_d = 1\text{--}30\text{ L kg}^{-1}$ , are much higher than usually observed for inorganic anions. This result was confirmed by through-diffusion experiments, but the  $K_d$  values obtained by fitting diffusion modelling were significantly lower than those measured in the batch experiments. The diffusion of organic and inorganic anions is mostly driven by anionic exclusion and, to a lesser extent, by a size dependency. Size effects may be evaluated for organics from diffusion values in water ( $D_0$ ) as a first approximation. Despite a significant sorption, the carboxylic acids display an anionic exclusion comparable to inorganic anions ( $0.1 < \Pi < 0.25$ ). The mobility of organics is not enhanced by clay-rock and “surface mobility” remains only evidenced for cations. The values obtained may be useful to estimate transport of small acids in natural environments such as sedimentary rocks.

## Acknowledgments

This work was partially financed by the “Agence Nationale pour la gestion des Déchets Radioactifs” (ANDRA). The authors thank Dr. Sebastien Savoye for useful discussion about diffusion experiments. We gratefully acknowledge Dr. Estela Reinoso-Maset and Dr. Scott Altmann for useful comments on the manuscript and for English improvement.

## Appendix A. Organic synthesis and additional data

Supplementary data associated with this article can be found, in the online version, at <http://dx.doi.org/10.1016/j.jhydrol.2014.02.002>.

## References

- Ali, M., Dzombak, D., 1996. Effects of simple organic acids on sorption of  $\text{Cu}^{2+}$  and  $\text{Ca}^{2+}$  on goethite. *Geochim. Cosmochim. Acta* 60, 291–304.
- Alliot, C., Vitorge, P., Bion, L., Mercier, F., 2005a. Effect of aqueous acetic, oxalic and carbonic acids on the adsorption of uranium(VI) on alpha-alumina. *New J. Chem.* 29, 1409–1415.
- Alliot, C., Bion, L., Mercier, F., Toulhoat, P., 2005b. Sorption of aqueous carbonic, acetic, and oxalic acids onto  $\alpha$ -alumina. *J. Colloid Interface. Sci.* 287, 444–451.
- Andra, 2005. Dossier 2005 Argile, Synthesis. Evaluation of the Feasibility of a Geological Repository in an Argillaceous Formation. Meuse/Haute-Marne site; Andra Report series 266.
- Arnarson, T.S., Keil, R.G., 2000. Mechanisms of pore water organic matter adsorption to montmorillonite. *Mar. Chem.* 71, 309–320.
- Bazer-bachi, F., Tevissen, E., Descostes, M., Grenut, B., Meier, P., Simonnot, M., Sardin, M., 2006. Characterization of iodide retention on Callovo-Oxfordian argillites and its influence on iodide migration. *Phys. Chem. Earth, Parts A/B/C* 31, 517–522.
- Bazer-bachi, F., Descostes, M., Tevissen, E., Meier, P., Grenut, B., Simonnot, M., Sardin, M., 2007. Characterization of sulphate sorption on Callovo-Oxfordian argillites by batch, column and through-diffusion experiments. *Phys. Chem. Earth, Parts A/B/C* 32, 552–558.
- Crank, J., 1975. *The Mathematics of Diffusion*, second ed. Oxford University Press, Clarendon Press, London.
- Darban, A.K., Foriero, A., Yong, R.N., 2000. Concentration effects of EDTA and chloride on the retention of trace metals in clays. *Eng. Geol.* 57, 81–94.
- Descostes, M., Tevissen, E., 2004. Definition of an equilibration protocol for batch experiments on Callovo-Oxfordian argillite. *Phys. Chem. Earth* 29, 79–90.
- Descostes, M., Blin, V., Bazer-Bachi, F., Meier, P., Grenut, B., Radwan, J., Schlegel, M.L., Buschaert, S., Coelho, D., Tevissen, E., 2008. Diffusion of anionic species in Callovo-Oxfordian argillites and Oxfordian limestones (Meuse/Haute-Marne, France). *Appl. Geochem.* 23, 655–677.
- Descostes, M., Pili, E., Felix, O., Frasca, B., Radwan, J., Juery, A., 2012. Diffusive parameters of tritiated water and uranium in chalk. *J. Hydrol.* 452–453, 40–50.
- Drouin, S., Boussafir, M., Robert, J.-L., Alberic, P., Durand, A., 2010. Carboxylic acid sorption on synthetic clays in sea water: in vitro experiments and implications for organo-clay behaviour under marine conditions. *Organ. Geochem.* 41 (2), 192–199.
- Duro, L., Grivé, M., Giffaut, E., 2012. Thermochimie, the ANDRA thermodynamic Database. In: *MRS Proceedings*, vol. 1475.
- Furukawa, K., Takahashi, Y., Sato, H., 2007. Effect of the formation of EDTA complexes on the diffusion of metal ions in water. *Geochim. Cosmochim. Acta* 71, 4416–4424.
- Gaucher, E.C., Blanc, P., Bardot, F., Braibant, G., Buschaert, S., Crouzet, C., Gautier, A., Girard, J.-P., 2006. Modelling the porewater chemistry of the Callovian-Oxfordian formation at a regional scale. *C. R. Geosci.* 338, 917–930.
- Gimmi, T., Kosakowski, G., 2011. How mobile are sorbed cations in clays and clay rocks? *Environ. Sci. Technol.* 45, 1443–1449.
- Gu, B., Chen, Z., Mccarthy, J.F., Divlison, E.S., Division, C., Ridge, O., 1994. Adsorption and desorption of natural organic matter on iron oxide: mechanisms and models. *Environ. Sci. Technol.* 28, 38–46.
- Hakonen, M., Ervanne, H., 2006. The Influence of Organic Cement Additives on Radionuclide Mobility A Literature Survey. Working Report 2006–06, POISVA OY.
- Hakem, N.L., Allen, P.G., Sylwester, E.R., 2001. Effect of EDTA on plutonium migration. *J. Radioanal. Nucl. Chem.* 250, 47–53.
- Huclier-markai, S., Landesman, C., Rogniaux, H., Monteau, F., Vinsot, A., Grambow, B., 2010. Non-disturbing characterization of natural organic matter (NOM) contained in clay rock pore water by mass spectrometry using electrospray and atmospheric pressure chemical ionization modes. *Rapid Commun. Mass Spectrom.* 24, 191–202.
- Hummel, W., Anderegg, G., Rao, L., Puigdomènech, I., Tochiyama, O., 2005. Chemical Thermodynamics. Chemical Thermodynamics of Compounds and Complexes of U, Np, Pu, Am, Tc, Se, Ni and Zr with selected organic ligands, OECD Nuclear Energy Agency, vol. 9. Elsevier B.V..
- Hwang, Y.S., Liu, J., Lenhart, J.J., Hadad, C.M., 2007. Surface complexes of phthalic acid at the hematite/water interface. *J. Colloid Interface Sci.* 307, 124–134.
- Kan, A.T., Fu, G., Tomson, M.B., 1994. Adsorption/desorption hysteresis in organic pollutant and soil/sediment interaction. *Environ. Sci. Technol.*, 059–067.
- Kang, S., Xing, B., 2007. Adsorption of dicarboxylic acids by clay minerals as examined by in situ ATR-FTIR and ex situ DRIFT. *Langmuir* 23, 7024–7031.
- Keith-Roach, M.J., 2008. The speciation, stability, solubility and biodegradation of organic co-contaminant radionuclide complexes: a review. *Sci. Tot. Environ.* 96, 1–11.
- Kubicki, J.D., Schroeter, L.M., Itoh, M.J., Nguyen, B.N., Apitz, S.E., 1999. Attenuated total reflectance Fourier-transform infrared spectroscopy of carboxylic acids adsorbed onto mineral surfaces. *Geochim. Cosmochim. Acta* 63, 2709–2725.
- Maes, N., Bruggeman, C., Govaerts, J., Martens, E., Salah, S., Van Gompel, M., 2011. A consistent phenomenological model for natural organic matter linked migration of Tc(IV), Cm(III), Np(IV), Pu(III/IV) and Pa(V) in the boom clay. *Phys. Chem. Earth, Parts A/B/C* 36, 1590–1599.
- Martens, E., Maes, N., Weetjens, E., Van Gompel, M., Van Ravestyn, L., 2010. Modelling of a large-scale in-situ migration experiment with 14 C-labelled natural organic matter in boom clay. *Radiochim. Acta* 98, 695–701.
- Melkior, T., Yahiaoui, S., Motellier, S., Thoby, D., Tevissen, E., 2005. Cesium sorption and diffusion in Bure mudrock samples. *Appl. Clay Sci.* 29, 172–186.
- Melkior, T., Yahiaoui, S., Thoby, D., Motellier, S., Barthes, V., 2007. Diffusion coefficients of alkaline cations in Bure mudrock. *Phys. Chem. Earth, Parts A/B/C* 32, 453–462.
- Mesuer, K., Fish, W., 1992. Chromate and oxalate adsorption on goethite. 1. Calibration of surface complexation models. *Environ. Sci. Technol.* 26, 2357–2364.
- Miller, A.W., Wang, Y., 2012. Radionuclide interaction with clays in dilute and heavily compacted systems: a critical review. *Environ. Sci. Technol.* 46, 1981–1994.
- Montarnal, P., Mugler, C., Colin, J., Descostes, M., Dimier, A., Jacquot, E., 2007. Presentation and use of a reactive transport code in porous media. *Phys. Chem. Earth, Parts A/B/C* 32, 507–517.
- Moridis, G.J., 1998. A set of semianalytical solutions for parameter estimation in diffusion cell experiments. *Sciences-New York*.
- Nogueira, F., Lopes, J., Silva, A., Goncalves, M., Anastacio, A., Sapag, K., Oliveira, L., 2009. Reactive adsorption of methylene blue on montmorillonite via an ESI-MS study. *Appl. Clay Sci.* 43, 190–195.
- Nowara, A., Burhenne, J., Spittler, M., 1997. Binding of fluoroquinolone carboxylic acid derivatives to clay minerals. *J. Agric. Food Chem.* 12, 1459.
- Pace, M.N., Mayes, M.A., Jardine, P.M., McKay, L.D., Yin, X.L., Mehlhorn, T.L., Liu, Q., Gürleyük, H., 2007. Transport of  $\text{Sr}^{2+}$  and  $\text{SrEDTA}^{2-}$  in partially-saturated and heterogeneous sediments. *J. Contam. Hydrol.* 91, 267–287.
- Parkhurst, D.L., Appelo, C.A.J., 1999. User's guide to PHREEQC (version 2) – a Computer Program for Speciation, Batch-reaction, One-Dimensional Transport, and Inverse Geochemical Calculations, US Geol. Surv. Water Resour. Invest. Rep. 99-4259.

- Persson, P., Nordin, J., Rosenqvist, J., Lfvgrn, L., Öhman, L.O., Sjöberg, S., 1998. Comparison of the adsorption of o-phthalate on boehmite ( $\gamma$ -AlOOH), aged  $\gamma$ -Al<sub>2</sub>O<sub>3</sub>, and goethite ( $\alpha$ -FeOOH). *J. Colloid Interface Sci.* 206, 250–266.
- Pignatello, J., 1999. The measurement and interpretation of sorption and desorption rates for organic compounds in soil media. *Adv. Agron.* 69, 1–73.
- Poinssot, C., Geckeis, H., 2012. Radionuclide behaviour in the natural environment. Woodhead Publishing Series in Energy No. 42.
- Read, D., Ross, D., Sims, R.J., 1998. The migration of uranium through Clashach Sandstone: the role of low molecular weight organics in enhancing radionuclide transport. *J. Contam. Hydrol.* 35, 235–248.
- Savoie, S., Goutelard, F., Beaucaire, C., Charles, Y., Fayette, A., Herbette, M., Larabi, Y., Coelho, D., 2011. Effect of temperature on the containment properties of argillaceous rocks: the case study of Callovo-Oxfordian claystones. *J. Contam. Hydrol.* 125, 102–112.
- Savoie, S., Frasca, B., Grenut, B., Fayette, A., 2012. How mobile is iodide in the callovo-oxfordian claystones under experimental conditions close to the in situ ones? *J. Contam. Hydrol.* 142–143C, 82–92.
- Schug, K., McNair, H.M., 2003. Adduct formation in electrospray ionization mass spectrometry II. Benzoic acid derivatives. *J. Chromat. A.* 985, 531–539.
- Shakir, K., Flex, H., Benyamin, K., 1993. Effect of complexing agents and surfactants on the sorption of Co(II) by kaolinite. *J. Radioanal. Nucl. Chem.* 173, 303–311.
- Smith, J.T., Comans, R.N.J., 1996. Modelling the diffusive transport and remobilisation of <sup>137</sup>Cs in sediments: The effects of sorption kinetics and reversibility. *Geochim. Cosmochim. Acta* 60 (6), 995–1004.
- Stockdale, A., Bryan, N.D., 2013. The influence of natural organic matter on radionuclide mobility under conditions relevant to cementitious disposal of radioactive wastes: a review of direct evidence. *Earth Sci. Rev.* 121, 1–17.
- Tits, J., Wieland, E., Bradbury, M.H., Eckert, P., Schaible, A., 2002. The Uptake of Eu (III) and Th(IV) by Calcite under Hyperalkaline Conditions, PSI Bericht 02-03, ISSN 1019-0643.
- Valencia, D.P., González, F.J., 2012. Estimation of diffusion coefficients by using a linear correlation between the diffusion coefficient and molecular weight. *J. Electr. Chem.* 681, 121–126.
- Van Brakel, J., Heertjes, P.M., 1974. Analysis of diffusion in macroporous media in terms of a porosity, a tortuosity, and a constrictivity factor. *J. Heat Mass Transfer* 17, 1093–1103.
- Wieland, B.E., Tits, J., Dobler, J.P., Spieler, P., 2002. The effect of  $\alpha$ -isosaccharinic acid on the stability of and Th (IV) uptake by hardened cement paste. *Radiochim. Acta* 90, 683–688.
- Zheng, Y., Zaoui, A., 2011. How water and counterions diffuse into the hydrated montmorillonite. *Solid State Ionics* 203, 80–85.
- Zhou, J., Lu, X., Wang, Y., Shi, J., 2002. Molecular dynamics study on ionic hydration. *Fluid Phase Equilib.* 194–197, 257–270.